

Frequency Characteristics of the Input Impedance of Meander Slow-wave System with Additional Shields

E. Metlevskis¹, R. Martavicius¹

¹Department of Electronic Systems, Vilnius Gediminas Technical University,
Naugarduko St. 41–422, LT-03227 Vilnius, Lithuania
edvardas.metlevskis@vgtu.lt

Abstract—A method for determination of input impedance of meander slow-wave system with additional shields is presented. It is based on a technique used for a calculation of frequency characteristics of helical slow-wave systems. The input impedance was determined at two ports: on the edge and in the centre of a system. S_{11} parameter is known as the input reflection coefficient, so system's input impedance in the lower frequencies can be determined by changing the signal source and load resistances until minimum value of S_{11} parameter is obtained. Using proposed method frequency characteristics of input impedance and S_{11} parameter of a meander slow-wave system with additional shields is analysed in Sonnet software.

Index Terms—Microwave integrated circuits, scattering parameters, impedance matching.

I. INTRODUCTION

Meander slow-wave systems are planar structures that can be easily manufactured using standard monolithic microwave integrated circuit (MMIC) fabrication technologies. Pass-band of such systems starts at low frequencies therefore they are widely used as delay lines and deflection systems [1]–[3]. Moreover due to their compact size meander-shape structures are used for design of antennas for wireless communications systems [4], [5], biomedical applications [6], digital video broadcasting [7] and radio frequency identification [8], [9]. Furthermore meander-shape conductors are applied for design of filters [10], [11], couplers [12] and phase shifters [13], [14].

Phase delay time of a typical meander slow-wave system is highly dependent on a frequency of propagating signal – the higher the frequency the higher the phase delay time. The reason for that is the frequency dependent electromagnetic interaction between adjacent meander strips. In order to reduce the electromagnetic interaction, additional shields are inserted between adjacent meander conductors and connected to an external shield by vias. As a rule, external shield is grounded. As a result of that a meander slow-wave system with loop-shape additional shields shown in Fig. 1 is created. A single conductor has a length of $2A$ and width w_1 . A gap between neighbouring conductors is denoted s_1 . Widths of an additional shield and a conductor connecting

adjacent meander strips are denoted w_2 and w_3 respectively. A gap between meander strip and additional shield is denoted s_2 .

Various methods are used for the analysis of meander slow-wave systems. Most commonly the multiconductor line method is chosen [15]. The drawback of this method is inability to evaluate ongoing processes on the edges of meander. Evaluation of ongoing processes can be done by using models which are based on numerical techniques [16]. In paper [17] using *Sonnet*® [18] software an impact of different topologies of meander edges on dispersion properties of meander slow-wave system is determined. However there is still a lack of information about input impedance and S-parameters of meander slow-wave systems with additional shields which is needed for evaluation of compatibility of a system with a signal tract. In this paper a method for determination of input impedance of meander slow-wave system with additional shields using *Sonnet*® software is presented. Also frequency characteristics of input impedance and S_{11} parameter are analysed.

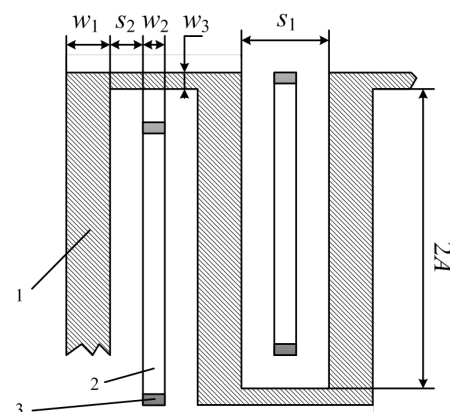


Fig. 1. Topology of meander slow-wave system with loop-shape additional shields: 1 – meander shape conductor; 2 – additional loop-shape shields; 3 – grounded via.

II. INPUT IMPEDANCE DETERMINATION TECHNIQUE

3D model of investigated meander slow-wave system with additional shields created with *Sonnet*® is shown in Fig. 2. Slow-wave system has a rectangular shape; it consists of 7 parallel conductors which are connected in a shape of meander and 8 additional shields which are connected by

vias at both ends to an external shield. Strips of a meander together with additional shields are placed on a dielectric plate with a thickness of h and permittivity of ϵ_r . Bottom of a plate is covered with metal which forms an external shield. Above the dielectric plate is air. Therefore cross-section of a system contains two layers of dielectric. Bottom layer has a permittivity of $\epsilon_r = 7.3$, top layer consists of air which has a relative dielectric permittivity of 1. Dimensions of a meander slow-wave system are: $2A = 20$ mm, $w_1 = 0.5$ mm, $w_2 = 0.25$ mm, $w_3 = 0.2$ mm, $h = 0.5$ mm, $s_1 = 0.65$ mm, $s_2 = 0.2$ mm. During the investigation perfect conductors were used. So investigated system has no loss.

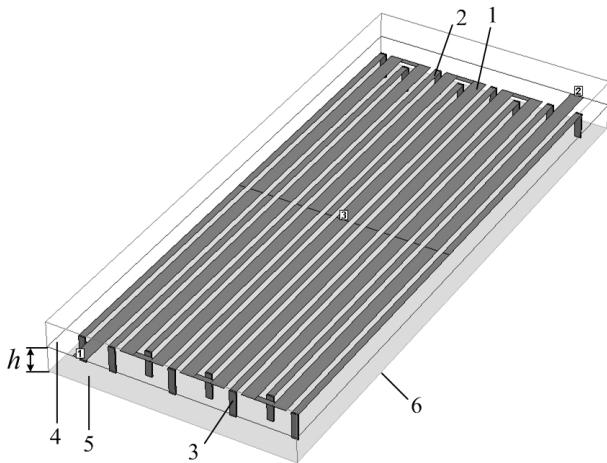
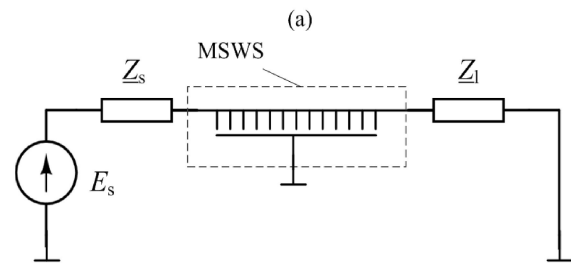
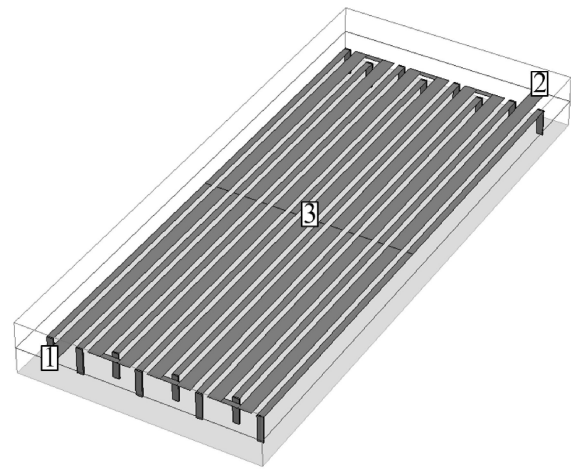


Fig. 2. 3D model of investigated meander slow-wave system with loop-shape additional shields created with *Sonnet*® software: 1 – meander shape conductor; 2 – additional shields; 3 – via; 4 – layer of air; 5 – dielectric substrate of thickness h ; 6 – grounded external shield.

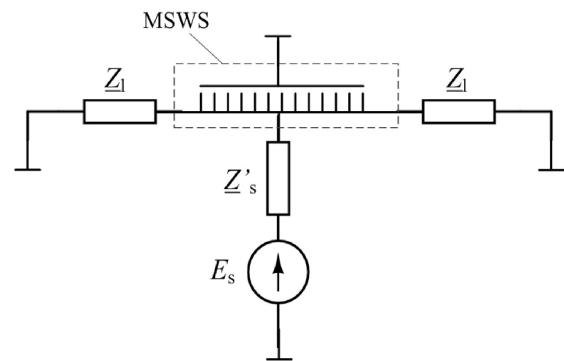
System's input impedance in the lower frequencies was determined by a technique used for a calculation of frequency characteristics of helical slow-wave systems which is described in [19]. The input impedance of meander slow-wave system with additional shields in the lower frequencies was determined at two ports: on the edge of a system which in Fig. 3(a) are denoted by numbers 1 and 2, and in the centre of a system which is denoted by number 3. A signal path developed for the determination of the input impedance in the lower frequencies on the edge of a system is shown in Fig. 3(b). It can be seen that reflections in the path with the slow-wave system do not exist if the internal resistance of the signal source and load resistance are matched with system's input impedance in the lower frequencies. Thus, at a selected low frequency f , system's input impedance can be determined by changing the signal source and load resistances until minimum value of S_{11} parameter is obtained. So when load and source resistances are matched with slow-wave system's impedance, least reflections are obtained since S_{11} parameter is known as the input reflection coefficient. In such way input impedance $Z_{IN}(f)$ in the lower frequencies on the edge of the slow-wave system is determined.

A signal path developed for the determination of the input impedance in the lower frequencies in the centre of a system is shown in Fig. 3(c). In such case a signal is sent through a port in the centre of a system while both ends of a system are loaded by resistances that are equal to slow-wave system's input impedance in the lower frequencies. Since signal is

sent simultaneously in both directions the resistance of signal source must be equal to half of the system's input impedance in the lower frequencies. Therefore it must be equal to the half of the load resistance $Z_s = Z_L/2$.



(b)



(c)

Fig. 3. Investigation of input impedance of meander slow-wave system with additional shields: (a) – ports at which input impedance was determined; A signal path developed for determination of the input impedance on the edge of a system (b) and in the centre of a system (c).

Equivalent circuit of a port in *Sonnet*® software is shown in Fig. 4. It is described by four parameters: resistance R , reactance X , inductance L and capacitance C . The values of these parameters can be changed. For that purpose in *Sonnet*® software a table similar to Table I is used for setting source and load resistances. During the investigation only resistance was changed. So $Z_s = R_s$, $Z_L = R_L$ and $R_s = R_L = Z_{LF}$. Obtained value of Z_{LF} is the input impedance in the lower frequencies of a meander slow-wave system with additional shields.

Frequency response of S_{11} parameter when determining input impedance in the lower frequencies on the edges of a meander slow-wave system with additional shields is shown

in Fig. 5. By default when analysis of a system is performed in *Sonnet*® software load and source resistances are set to 50 Ω . Frequency response of S_{11} parameter corresponding to such values is shown in Fig. 5 by curve 1. Curve 2 represents a frequency response of S_{11} parameter when load and source resistances are matched to the system's input impedance. It can be seen that when load and source resistances are matched S_{11} parameter in the lower frequencies has a value that is near to 0.

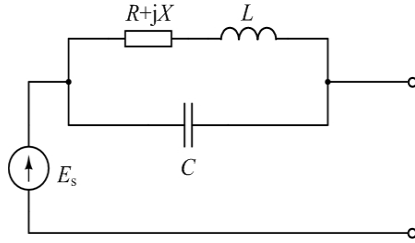


Fig. 4. Equivalent circuit of a port in *Sonnet*® software.

TABLE I. SETTINGS FOR SOURCE AND LOAD RESISTANCES.

Port number	Resistance (Ohms)	Reactance (Ohms)	Inductance (nH)	Capacitance (pF)
1	50	0	0	0
2	50	0	0	0
3	25	0	0	0

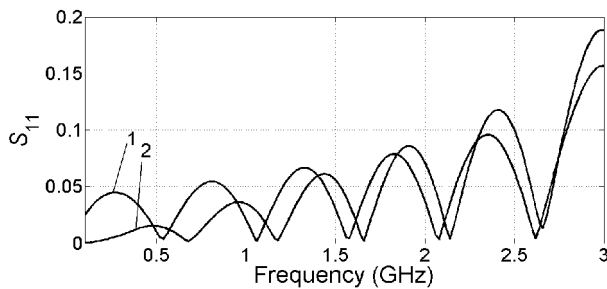


Fig. 5. Frequency response of S_{11} parameter when determining input impedance in the lower frequencies on the edges of a meander slow-wave system with additional shields: 1 – when $R_s = R_l = 50 \Omega$; 2 – when load and source resistances are matched to the system's input impedance $R_s = R_l = 48 \Omega$.

Frequency response of S_{11} parameter when determining input impedance in the lower frequencies in the centre of a meander slow-wave system with additional shields is shown in Fig. 6. Here curve 1 represents a case when load resistance $R_l = 50 \Omega$ and source resistance $R_s = 25 \Omega$ (Table I). Curve 2 represents a frequency response of S_{11} parameter when load and source resistances are matched. Herein a decrease of S_{11} parameter in the lower frequencies can be observed when load and source resistances are matched to the system's input impedance.

III. FREQUENCY CHARACTERISTICS OF INPUT IMPEDANCE OF WIDE-BAND MEANDER SLOW-WAVE SYSTEM

Input impedance of meander slow-wave system was determined from S_{11} parameter. After analysis of a system in *Sonnet*® software, S_{11} parameters are obtained. Then the input impedance can be calculated using following formula

$$Z_{IN} = Z_l \left(\frac{1 + S_{11}}{1 - S_{11}} \right), \quad (1)$$

where Z_l is matched load resistance. Generally input impedance Z_{IN} is complex

$$\underline{Z}_{IN} = R_{IN} + jX_{IN}. \quad (2)$$

So from the complex value of input impedance resistance

$$R_{IN} = \text{Re}[\underline{Z}_{IN}], \quad (3)$$

and reactance

$$X_{IN} = \text{Im}[\underline{Z}_{IN}] \quad (4)$$

can be obtained.

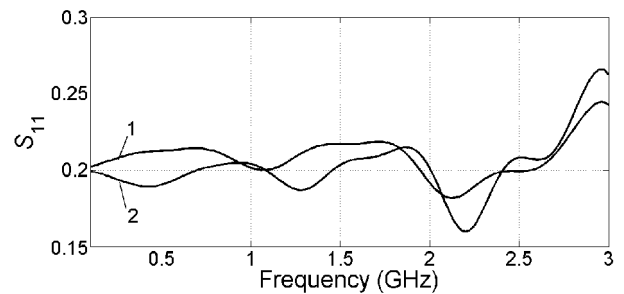


Fig. 6. Frequency response of S_{11} parameter when determining input impedance in the lower frequencies in the centre of a meander slow-wave system with additional shields: 1 – when $R_l = 50 \Omega$, $R_s = 25 \Omega$; 2 – when load and source resistances are matched to the system's input impedance $R_l = 46.7 \Omega$, $R_s = 23.35 \Omega$.

Results of investigation are presented in Fig. 7 and Fig. 8. In Fig. 7 a frequency response of the input impedance on the edges of a meander slow-wave system with additional shields is shown. Curve 1 represents a resistance R and curve 2 a reactance X of the input impedance. It can be seen that resistance of the input impedance on the edges of investigated system remains almost constant in a frequency range up to 1.5 GHz and has a value of 48 Ω . In the higher frequencies fluctuations of the input impedance can be observed. Fluctuations are caused by the changes of the structure of electromagnetic field on the edges of the system and also by electromagnetic interaction between adjacent meander strips. Moreover it should be noted that reactance of the input impedance has a very small value on the whole investigated frequency range so the input impedance on the edges of a meander slow-wave system with additional shields is purely resistive.

A frequency response of the input impedance in the center of a meander slow-wave system is shown in Fig. 8. Here it can be seen that the input impedance in the center of investigated system remains constant in the wider frequency range up to 2 GHz. It can be explained by the fact that in this point of a system edge effects have no influence on the input impedance. Input impedance in the centre of a system fluctuates due to electromagnetic interaction between adjacent meander strips. Value of the input impedance in the lower frequencies is the same as on the edges of a system. Reactance of the input impedance in the centre of the system as well as on the edges also has very small value so the input impedance in this part of a system is purely resistive too.

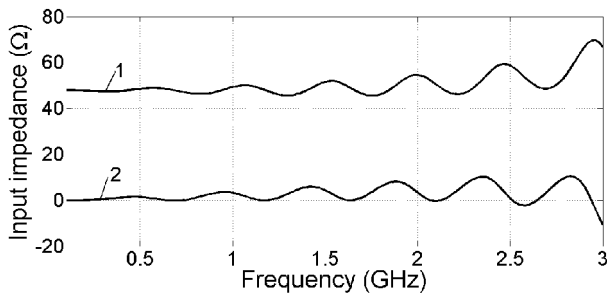


Fig. 7. Frequency response of the input impedance on the edges of a meander slow-wave system with additional shields: 1 – resistance R ; 2 – reactance X .

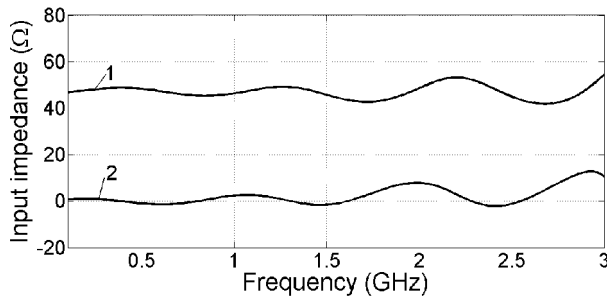


Fig. 8. Frequency response of the input impedance in the center of a meander slow-wave system with additional shields: 1 – resistance R ; 2 – reactance X .

IV. CONCLUSIONS

1. Presented method is suitable for the determination of the input impedance on the edges and in the centre of a meander slow-wave system with additional shields.

2. To determine the input impedance of the meander slow-wave system it is sufficient to match load and source resistances in the lower frequencies and calculate frequency characteristics from S_{11} parameter.

3. Input impedance on the edges of investigated meander slow-wave system with additional shields is almost constant in the frequency range up to 1.5 GHz. Reactance of the input impedance has a very small value on the whole investigated frequency range so the input impedance on the edges of a meander slow-wave system with additional shields is purely resistive.

4. Input impedance in the centre of a meander slow-wave system with additional shields is almost constant in the frequency range up to 2 GHz and a value of the input impedance in the lower frequencies is the same as on the edges of a system. Input impedance in this part of a system is also purely resistive.

REFERENCES

- [1] W. S. Chang, C. Y. Chang, "A high slow-wave factor microstrip structure with simple design formulas and its application to microwave circuit design", *IEEE Trans. on Microwave Theory and Techniques*, vol. 60, no. 11, pp. 3376–3383, Nov. 2012. [Online]. Available: <http://dx.doi.org/10.1109/TMTT.2012.2216282>
- [2] M. Sumathy, L. Christie, S. K. Datta, L. Kumar, "Analysis of a W-band meander-line slow-wave structure for millimetre-wave traveling-wave tubes", in *IEEE 13th Int. Vacuum Electronics Conf.*, 2012, pp. 461–462.
- [3] C. Chen, "Effect of structural parameters on high frequency characteristics of microstrip meander-line slow-wave structure", *Applied Mechanics and Materials*, vol. 241–244, pp. 698–702, Dec. 2012. [Online]. Available: <http://dx.doi.org/10.4028/www.scientific.net/AMM.241-244.698>
- [4] C. G. M. Ryan, G. V. Eleftheriades, "Two compact, wideband, and decoupled meander line antennas based on metamaterial concepts", *IEEE Antennas and Wireless Propagation Letters*, vol. 11, pp. 1277–1280, 2012. [Online]. Available: <http://dx.doi.org/10.1109/LAWP.2012.2225134>
- [5] D. M. Elsheikh, A. M. E. Safwat, "Meander line-loaded planar monopole antennas", *Microwave and Optical Technology Letters*, vol. 54, no. 8, pp. 1851–1854, Aug. 2012. [Online]. Available: <http://dx.doi.org/10.1002/mop.26939>
- [6] O. Diop *et al.*, "Planar antennas on integrated passive device technology for biomedical applications", in *IEEE Int. Workshop on Antenna Technology*, 2012, pp. 217–220.
- [7] M. A. C. Nieminen, A. Sharaiha, S. Collardey, K. Mahdjoubi, "An electrically small frequency reconfigurable antenna for DVB-H", in *IEEE Int. Workshop on Antenna Technology*, 2012, pp. 245–248.
- [8] M. Kanesan, D. V. Thiel, S. G. O'Keefe, "The effect of lossy dielectric objects on a UHF RFID meander line antenna", in *IEEE Antennas and Propagation Society Int. Symposium*, 2012, pp. 1–2.
- [9] P. Wongsiritorn, T. Pumpoung, C. Phongcharoenpanich, K. Nuangwongsa, S. Kosulvit, "Meander-line antenna with arc structure for UHF-RFID Tag", in *Int. Symposium on Intelligent Signal Processing and Communications Systems*, 2011, pp. 1–4.
- [10] S. Lin, H. Cui, L. Wu, W. Wang, X. Sun, "Design of broadside-coupled parallel line millimetre wave filters by standard 0.18- μ m complementary metal oxide semiconductor technology", *IET Microwaves, Antennas & Propagation*, vol. 6, no. 1, pp. 72–78, Jan. 2011. [Online]. Available: <http://dx.doi.org/10.1049/iet-map.2011.0024>
- [11] K. W. Hsu, W. H. Tu, "Sharp rejection quad-band bandpass filter using meandering structure", *Electronics Letters*, vol. 48, no. 15, pp. 935–937, 2012. [Online]. Available: <http://dx.doi.org/10.1049/el.2012.1735>
- [12] H. C. Chiu, C. H. Lai, T.-G. Ma, "Miniaturized rat-race coupler with out-of-band suppression using double-layer synthesized coplanar waveguides", in *IEEE MTT-S Int. Microwave Symposium Digest*, 2012, pp. 1–3.
- [13] Jing Wu *et al.*, "Compact, low-loss, wideband, and high-power handling phase shifters with piezoelectric transducer-controlled metallic pertruber", in *IEEE Trans. on Microwave Theory and Techniques*, vol. 60, no. 6, pp. 1587–1594, 2012. [Online]. Available: <http://dx.doi.org/10.1109/TMTT.2012.2189240>
- [14] A. Chakraborty, A. Kundu, S. Dhar, S. Maity, S. Chatterjee, B. Gupta, "Compact K-band distributed RF MEMS phase shifters based on high-speed switched capacitors", in *11th Mediterranean Microwave Symposium*, 2011, pp. 25–28.
- [15] S. Mikucionis, V. Urbanavicius, "Synthesis of six-conductors symmetrically coupled microstrip line, operating in a normal mode", *Elektronika ir Elektrotechnika (Electronics and Electrical Engineering)*, no. 4, pp. 47–52, 2011.
- [16] A. Krukoniis, V. Urbanavicius, "Investigation of microstrip lines dispersion by the FDTD method", *Elektronika ir Elektrotechnika (Electronics and Electrical Engineering)*, no. 9, pp. 51–54, 2011.
- [17] E. Metlevskis, R. Martavicius, "Calculation of characteristics of meander slow-wave system with additional shields", in *Proc. XXII Int. Conf. on Electromagnetic Disturbances*, Vilnius, 2012, pp. 87–90.
- [18] Sonnet Software. *EM Analysis and Simulation – High Frequency Electromagnetic Software Solutions*. [Online]. Available: <http://www.sonnetsoftware.com/>
- [19] S. Staras, R. Martavicius, J. Skudutis, V. Urbanavicius, V. Daskevicius, *Wide-Band Slow-Wave Systems: Simulation and Applications*. New York: CRC Press, 2012, ch. 5.